A Split Stretch/Slip Formulation for Routed Cable Joints

Newton Developers

May 2026

Abstract

This note describes the reduced routed-cable model used by Newton's tendon solver for massless cables over attachments, zero-radius pinholes, and finite-radius rolling pulleys. The formulation separates the cable solve into three local mechanisms: unilateral free-span stretch, capstan slip represented as rest-length redistribution, and a capstan-limited rolling spin row. The same rows are used by the XPBD solver and by the VBD rigid-body path. This document states the equations of motion, the exact constraint rows, and the rest-length projection derived directly from the Euler–Eytelwein capstan equation.

1 Model

Let a tendon be an ordered sequence of links $i = 0, \dots, n-1$. Consecutive links define free spans $s = 0, \dots, n-2$. Each link is attached to a rigid body b_i and has one of three types:

$$\texttt{ATTACHMENT}, \qquad \texttt{PINHOLE}, \qquad \texttt{ROLLING}.$$

Each free span stores a mutable rest length r_s, compliance c_s, damping d_s, and stretch multiplier λ_s. The rest-length distribution is the state that records how much cable material is assigned to each free span.

For body b, let

$$q_b = (p_b, Q_b), \qquad v_b = (u_b, \omega_b),$$

where p_b is translation, $Q_b \in SO(3)$ is orientation, u_b is linear velocity, and ω_b is angular velocity. A body-local point o has world position

$$x_b(o) = p_b + Q_b o.$$

Let c_b^0 be the local center of mass and $x_b^c = p_b + Q_b c_b^0$ its world position. The velocity of $x = x_b(o)$ is

$$\dot{x} = u_b + \omega_b \times (x - x_b^c).$$

2 Equations of Motion and Discrete Projection

The unconstrained rigid-body dynamics can be written in generalized velocity form as

$$M(q)\dot{v} = f_{\text{ext}}(q, v, t) + J(q, r)^{\mathsf{T}} \tau, \tag{1}$$

where M is block-diagonal in body space, J contains the active cable rows, r is the vector of free-span rest lengths, and τ are row impulses or forces depending on time discretization.

Newton applies the cable model as local position/velocity projections. After external integration predicts $(q^\star, v^\star)$, each active row computes an increment $\Delta\lambda$ and applies the body-space impulse

$$\Delta p_b = J_{b,v}^{\mathsf{T}} \Delta\lambda, \qquad \Delta\ell_b = J_{b,\omega}^{\mathsf{T}} \Delta\lambda.$$

The velocity increment is

$$\Delta u_b = m_b^{-1} \Delta p_b, \qquad \Delta\omega_b = I_b^{-1} \Delta\ell_b,$$

using the same effective inverse mass and inverse inertia arrays as the solver path. The pose is advanced by the velocity increment over the substep h. For rigid-limit rows $c_s \to 0$, the stretch constraints satisfy the unilateral complementarity conditions

$$C_s(q, r_s) \le 0, \qquad \lambda_s \ge 0, \qquad \lambda_s C_s(q, r_s) = 0. \tag{2}$$

Finite compliance replaces this hard complementarity with the XPBD row below.

3 Route Update

For an attachment or pinhole, the route point is simply the body-local point transformed to world space. For a rolling link with center g, radius R, axis a, and orientation sign $\sigma \in \{-1, +1\}$, the tangent point from an external point p is computed in the plane orthogonal to a.

Let

$$d = g - p, \qquad \bar{d} = d - (d \cdot a)a, \qquad u = \frac{\bar{d}}{\|\bar{d}\|}, \qquad v = a \times u.$$

For $\|\bar{d}\| > R$, define

$$\phi = \arcsin\left(\min\left(\frac{R}{\|\bar{d}\|}, 1\right)\right), \qquad \psi = \begin{cases} -\pi/2 - \phi, & \sigma > 0, \\ \pi/2 + \phi, & \sigma < 0. \end{cases}$$

The tangent point is

$$x_{\tan} = g + R(\cos\psi\, u + \sin\psi\, v). \tag{3}$$

For a span between two rolling links, the two tangent points are iterated to consistency. A pure spin about the circular pulley axis does not change these tangent points; this is why the stretch row removes the spin-axis angular component.

When a rolling contact point moves from x_{old} to x_{new} on the pulley surface, the signed surface transfer used by the route update is

$$\Delta\ell = R\sigma\ \operatorname{atan2}(((u_{\text{new}} \times u_{\text{old}}) \cdot a), u_{\text{old}} \cdot u_{\text{new}}), \tag{4}$$

where u_{old} and u_{new} are the normalized radial vectors from the pulley center, projected into the pulley plane. The signed transfer is applied to the adjacent span rest length with the capstan factor

$$\alpha = \exp(\operatorname{clamp}(\mu\theta, 0, 20)), \qquad \beta = \frac{\alpha - 1}{\alpha + 1}, \tag{5}$$

so that $\mu = 0$ gives no surface drag and high friction approaches the no-slip surface-transfer limit.

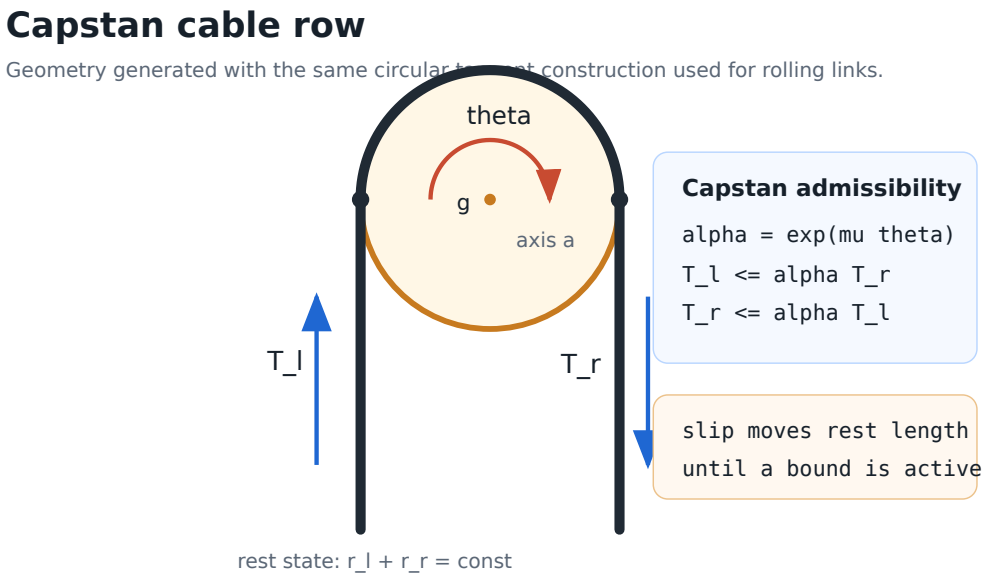

Figure 1: A single capstan row. The circular route update supplies the tangent points and wrap angle θ. The stretch rows carry the adjacent span tensions T_l, T_r, while slip changes only the rest-length distribution subject to $r_l + r_r = \text{const}$ and the capstan band.

4 Free-Span Stretch Row

Span s runs from left endpoint x_s^L on body b_L to right endpoint x_s^R on body b_R. Its geometric length, unit direction, and unilateral stretch constraint are

$$L_s = \|x_s^R - x_s^L\|, \qquad n_s = \frac{x_s^R - x_s^L}{\max(L_s, \varepsilon)}, \qquad C_s(q, r_s) = L_s - r_s \le 0. \tag{6}$$

If $C_s \le 0$, the span is slack: the row is inactive, λ_s is reset to zero, and the span contributes no tension.

For an active taut span, the translational Jacobian blocks are

$$J_{L,v} = -n_s, \qquad J_{R,v} = n_s. \tag{7}$$

Let

$$\rho_L = x_s^L - x_{b_L}^c, \qquad \rho_R = x_s^R - x_{b_R}^c.$$

The unprojected angular blocks are

$$\widehat{J}_{L,\omega} = -\rho_L \times n_s, \qquad \widehat{J}_{R,\omega} = \rho_R \times n_s. \tag{8}$$

For an endpoint that lies on a rolling link with world axis a, the stretch row removes the spin-axis component:

$$J_\omega = \Pi_a^\perp \widehat{J}_\omega, \qquad \Pi_a^\perp = I - aa^\mathsf{T}. \tag{9}$$

For attachments and pinholes, $J_\omega = \widehat{J}_\omega$. Equation (9) is a modeling choice, not a numerical tweak: pulley spin does not change the route tangent geometry, so the stretch row should not accidentally impose a no-slip pulley constraint.

The row velocity and effective inverse mass are

$$\dot{C}_s = J_{L,v} \cdot u_L + J_{L,\omega} \cdot \omega_L + J_{R,v} \cdot u_R + J_{R,\omega} \cdot \omega_R, \tag{10}$$

$$w_s = J_s M^{-1} J_s^{\mathsf{T}}. \tag{11}$$

Written in body blocks,

$$w_s = m_L^{-1} \|J_{L,v}\|^2 + J_{L,\omega}^{\mathsf{T}} I_L^{-1} J_{L,\omega} + m_R^{-1} \|J_{R,v}\|^2 + J_{R,\omega}^{\mathsf{T}} I_R^{-1} J_{R,\omega}. \tag{12}$$

Newton's implemented XPBD increment is

$$\gamma_s = c_s d_s, \qquad \Delta\lambda_s = -\frac{C_s + c_s \lambda_s + \gamma_s \dot{C}_s}{(h + \gamma_s) w_s + c_s / h}. \tag{13}$$

The solver stores both $\lambda_s \leftarrow \lambda_s + \Delta\lambda_s$ and the latest $\Delta\lambda_s$. The latter is used by the rolling spin row.

The stretch row applies the impulse-like body deltas

$$\Delta P_{b_L} = J_{L,v}^{\mathsf{T}} \Delta\lambda_s, \quad \Delta L_{b_L} = J_{L,\omega}^{\mathsf{T}} \Delta\lambda_s, \quad \Delta P_{b_R} = J_{R,v}^{\mathsf{T}} \Delta\lambda_s, \quad \Delta L_{b_R} = J_{R,\omega}^{\mathsf{T}} \Delta\lambda_s. \tag{14}$$

Relaxation multiplies these deltas before they are accumulated.

5 Capstan Slip as Rest-Length Projection

For a guide g between a left span l and right span r, define taut extensions and tension estimates

$$e_l = \max(L_l - r_l, 0), \qquad e_r = \max(L_r - r_r, 0), \qquad T_l = \frac{e_l}{\max(c_l, \varepsilon)}, \qquad T_r = \frac{e_r}{\max(c_r, \varepsilon)}. \tag{15}$$

For a pinhole, the bend angle is

$$\theta = \operatorname{atan2}(\|d_{\text{in}} \times d_{\text{out}}\|, d_{\text{in}} \cdot d_{\text{out}}), \tag{16}$$

where d_{in} is the incoming unit cable direction into the pinhole and d_{out} is the outgoing unit direction. For a rolling link,

$$\theta = |\operatorname{atan2}((u_l \times u_r) \cdot a,\ u_l \cdot u_r)|, \tag{17}$$

where u_l and u_r are the normalized radial vectors from the pulley center to the two tangent points, projected into the pulley plane.

The Euler–Eytelwein capstan law gives the admissible static tension band

$$T_l \le \alpha T_r, \qquad T_r \le \alpha T_l, \qquad \alpha = \exp(\operatorname{clamp}(\mu\theta, 0, 20)). \tag{18}$$

Equivalently,

$$\frac{1}{\alpha} \le \frac{T_l}{T_r} \le \alpha. \tag{19}$$

Inside this band the guide sticks and the adjacent rest lengths are unchanged. Outside the band, rest length is transferred between the two spans while preserving

$$r_l' + r_r' = r_l + r_r. \tag{20}$$

5.1 Left Side Too Tight

If $T_l > \alpha T_r$, the active capstan boundary after projection is

$$\frac{e'_l}{c_l} = \alpha \frac{e'_r}{c_r}. \tag{21}$$

Conservation means

$$r'_l = r_l + \delta, \qquad r'_r = r_r - \delta,$$

so the taut extensions become

$$e'_l = e_l - \delta, \qquad e'_r = e_r + \delta.$$

Substituting these directly into (21) gives

$$\frac{e_l - \delta}{c_l} = \alpha \frac{e_r + \delta}{c_r}.$$

Solving for the rest-length transfer,

$$\delta_l = \frac{c_r e_l - \alpha c_l e_r}{c_r + \alpha c_l}. \tag{22}$$

The implementation clamps

$$\delta = \mathrm{clamp}(\delta_l, 0, r_r - r_{\min}),$$

then applies

$$r_l \leftarrow r_l + \delta, \qquad r_r \leftarrow r_r - \delta.$$

5.2 Right Side Too Tight

If $T_r > \alpha T_l$, the active boundary is

$$\frac{e'_r}{c_r} = \alpha \frac{e'_l}{c_l}. \tag{23}$$

Now

$$r'_l = r_l - \delta, \qquad r'_r = r_r + \delta,$$

and therefore

$$e'_l = e_l + \delta, \qquad e'_r = e_r - \delta.$$

Substitution into (23) gives

$$\frac{e_r - \delta}{c_r} = \alpha \frac{e_l + \delta}{c_l},$$

so

$$\delta_r = \frac{c_l e_r - \alpha c_r e_l}{c_l + \alpha c_r}. \tag{24}$$

The implementation clamps

$$\delta = \mathrm{clamp}(\delta_r, 0, r_l - r_{\min}),$$

then applies

$$r_l \leftarrow r_l - \delta, \qquad r_r \leftarrow r_r + \delta.$$

Equations (22) and (24) are the desired rest-length distribution derived directly from the capstan equation. The capstan equation supplies the active boundary; rest-length conservation supplies the update structure.

6 Spin Coupling from the Same Capstan Projection

The capstan angle θ in (18) is the geometric wrap or bend angle. It is not the pulley spin angle. For a circular pulley, pure spin about the axle does not change the tangent points and therefore does not change θ. Pulley spin enters through surface travel. Let ϕ be the pulley spin angle, and choose the sign convention that a positive scalar transfer δ moves cable material from the left free span to the right free span:

$$r_l' = r_l - \delta, \qquad r_r' = r_r + \delta.$$

The rolling no-slip candidate over one substep is then

$$\delta_0 = \delta_{\text{geom}} + R\,\Delta\phi, \tag{25}$$

where δ_{geom} is the signed tangent-point surface transfer from the route update and $R\Delta\phi$ is the rim travel caused by pulley spin. This candidate gives

$$r_l^\star = r_l - \delta_0, \qquad r_r^\star = r_r + \delta_0, \tag{26}$$

and therefore

$$e_l^\star = \max(L_l - r_l^\star, 0), \qquad e_r^\star = \max(L_r - r_r^\star, 0), \tag{27}$$

$$T_l^\star = \frac{e_l^\star}{c_l}, \qquad T_r^\star = \frac{e_r^\star}{c_r}. \tag{28}$$

The no-slip rolling update is statically admissible exactly when the candidate tensions satisfy the capstan band:

$$\frac{1}{\alpha} \le \frac{T_l^\star}{T_r^\star} \le \alpha. \tag{29}$$

If (29) holds, static friction can support the candidate and $\delta = \delta_0$. If it does not hold, slip occurs and δ is projected back to the active capstan boundary using (22) or (24). In this sense, the rest-length update and the rolling no-slip/slip decision are both obtained from the same capstan equation: the spin angle only supplies the no-slip transfer candidate through $R\Delta\phi$.

The corresponding angular form follows by rewriting the capstan band as a bound on the tension difference. From $T_l = \alpha T_r$,

$$\frac{T_l - T_r}{T_l + T_r} = \frac{\alpha - 1}{\alpha + 1},$$

so the symmetric capstan cone is

$$|T_r - T_l| \le \beta(T_r + T_l), \qquad \beta = \frac{\alpha - 1}{\alpha + 1}. \tag{30}$$

The tangential force imbalance on a circular pulley is $T_r - T_l$, so the capstan-limited spin torque is

$$\tau_\phi = R\ \text{clamp}(T_r - T_l,\ -\beta(T_l + T_r),\ \beta(T_l + T_r))\,. \tag{31}$$

For a scalar spin inertia I_ϕ, the spin equation of motion is

$$I_\phi \dot{\omega}_\phi = \tau_\phi + \tau_{\text{ext}}, \tag{32}$$

and a simple discrete angular impulse update is

$$\Delta\omega_\phi = h I_\phi^{-1} \tau_\phi. \tag{33}$$

Equations (25)–(33) are a useful target formulation: capstan friction chooses between the no-slip surface-transfer candidate and an active-boundary slip projection, while the same capstan cone supplies the admissible pulley spin torque.

7 Rolling Spin-Axis Row

The stretch row intentionally removed pulley spin coupling in (9). A rolling link therefore receives a separate angular correction, admitted only to the extent allowed by the same capstan cone. The current implementation uses an impulse-style approximation to (31): it reconstructs the spin-axis correction that the neighboring stretch rows would have applied, then gates that correction by the difference cone (30).

The symmetric difference/sum form of the capstan band is

$$|T_l - T_r| \le \beta(T_l + T_r), \qquad \beta = \frac{\alpha - 1}{\alpha + 1}. \tag{34}$$

This is the same cone as (30).

For a rolling guide body with axis a, define

$$s_g = \min\left(1,\ \frac{\beta(T_l + T_r)}{\max(|T_l - T_r|, \varepsilon)}\right). \tag{35}$$

If the adjacent stretch rows had kept the spin-axis term, their angular corrections on the pulley would have contained

$$A_l = aa^{\mathsf{T}}\left((x_l^+ - x_g^c) \times n_l\right)\Delta\lambda_l\rho, \tag{36}$$

$$A_r = aa^{\mathsf{T}}\left(-(x_r^- - x_g^c) \times n_r\right)\Delta\lambda_r\rho, \tag{37}$$

where ρ is the relaxation factor, x_l^+ is the left span endpoint on the pulley, x_r^- is the right span endpoint on the pulley, x_g^c is the pulley body center of mass, and n_l, n_r are the left and right span directions.

The implemented rolling spin row applies the pure angular body delta

$$\Delta L_g^{\text{spin}} = \beta\, s_g\,(A_l + A_r), \qquad \Delta P_g^{\text{spin}} = 0. \tag{38}$$

This row has no independent multiplier in the current implementation. It uses the lagged stretch increments $\Delta\lambda_l, \Delta\lambda_r$ as the candidate no-slip rolling correction and gates that correction by the capstan cone. The limiting cases are:

$$\mu = 0 \Rightarrow \beta = 0 \quad \text{(no pulley spin grip)},$$

$$\mu \to \infty \Rightarrow \beta \to 1 \quad \text{(no-slip rolling limit)}.$$

8 Hysteresis

Because r_l and r_r are persistent state, the capstan projection reproduces static capstan hysteresis without requiring distinct static and kinetic coefficients. Consider a fixed left endpoint, a rolling guide, and a driven right endpoint. During loading, T_r increases. When

$$T_r > \alpha T_l,$$

equation (24) transfers rest length from left to right:

$$r_l \downarrow, \qquad r_r \uparrow .$$

The left endpoint has not moved, but the left span has shorter rest length, so the fixed side develops tension. On that loading slip boundary,

$$T_r/T_l = \alpha.$$

During unloading, the previous rest-length distribution remains latched while the tensions stay inside the capstan band. Once the opposite boundary is violated,

$$T_l > \alpha T_r,$$

equation (22) reverses the rest-length transfer and the unloading branch follows

$$T_l/T_r = \alpha.$$

The area between these two branches is the hysteresis band.

9 XPBD and VBD Integration

The XPBD tendon iteration is:

1. update route contacts and rolling/pinhole rest-length transfer,
2. solve each active free-span stretch row using (13),
3. solve each rolling spin-axis row using (38).

The VBD rigid-body path calls the same route update, stretch row, and rolling spin row inside the rigid iteration, using VBD's effective inverse mass and inverse inertia arrays. There is no separate VBD global length force and no separate tendon Hessian model for routed cables; VBD regularizes the rigid solve while reusing the same cable rows as XPBD.

10 Implementation Map

The equations above correspond to the current Newton implementation as follows:

Equation or mechanism	Implementation
Route tangent update and surface transfer	`newton/_src/solvers/tendon_kernels.py` `update_tendon_attachments`
Stretch row (13)	`newton/_src/solvers/xpbd/tendon_kernels.py` `solve_tendon_stretch`
Pinhole and rolling rest-length projection	`newton/_src/solvers/tendon_kernels.py` `update_tendon_attachments`
Rolling spin row (38)	`newton/_src/solvers/xpbd/tendon_kernels.py` `solve_tendon_slip`
VBD routed-tendon projection	`newton/_src/solvers/vbd/solver_vbd.py` `_project_tendon_constraints`

11 Limitations

This is a reduced massless cable model, not a resolved rope/contact model. It does not represent distributed cable mass, bending stiffness, contact patch pressure, or geodesic rerouting over arbitrary geometry. The pinhole and rolling capstan laws use local bend or wrap angle as the reduced contact measure. Displacement-driven force benchmarks require compliance somewhere in the system: cable compliance, actuator compliance, or a load-cell model.